

# Linear Semibridging Carbonyls. 6. Structure and Bonding in the Dimers of 17-Electron Tantalum Hexacarbonyl and Tetracarbonyl Diphosphine

Thomas F. Miller III, Douglas L. Strout, and Michael B. Hall\*

Department of Chemistry, Texas A&M University, College Station, Texas 77843-3255

Received February 27, 1998

The geometric and electronic structures of the 17-electron, metal-centered radicals  $\text{Ta}(\text{CO})_6$  and  $\text{Ta}(\text{CO})_4(\text{PH}_2\text{CH}_2\text{CH}_2\text{PH}_2)$  and the corresponding dimers were studied by density functional theory. For the monomer, a nearly octahedral structure was determined and calculated to have frequencies that are in good agreement with those observed in the experimental work. Additional calculations led to the determination of a  $[\text{Ta}(\text{CO})_6]_2$  dimer that was energetically bound with respect to the monomeric species. Inclusion of the bidentate phosphine ligands in various relative orientations resulted in several energetically competitive chelated dimers. In all of the stable dimers, linear semibridging carbonyls are supporting a weak, delocalized Ta–Ta interaction.

## Introduction

Whereas the metal-centered radical  $\text{V}(\text{CO})_6$  was first observed over 35 years ago, the isoelectronic niobium and tantalum hexacarbonyls have yet to be unambiguously observed.<sup>1</sup> In a recent effort by Koeslag et al.<sup>2</sup> to explore analogues of the  $\text{Ta}(\text{CO})_6$  complex, the 17-electron, metal-centered radical  $\text{Ta}(\text{CO})_4(\text{dppe})$  ( $\text{dppe} = \text{Ph}_2\text{PCH}_2\text{CH}_2\text{PPh}_2$ ) was isolated and characterized. Infrared, Raman, and EPR spectroscopy and magnetic susceptibility revealed that the monomer dimerized to  $\text{Ta}_2(\text{CO})_8(\text{dppe})_2$  in both solution and the solid state. Furthermore, these spectroscopic measurements suggested the presence of bridging carbonyls and anti-ferromagnetic coupling in the dimers.

Variance in the frequencies of CO stretching in the solution-phase IR spectra at 298 and 243 K mark the presence of a temperature-dependent equilibrium between the monomer and dimer. The lower-frequency absorptions exhibited by the lower-temperature spectrum indicate that dimerization is slightly thermodynamically favorable. The solid-state IR spectrum clearly shows at least two absorptions in the bridging carbonyl region, 1795–1830  $\text{cm}^{-1}$ , along with differences from the terminal carbonyl range of the room-temperature solution spectrum. Thus, the dimer appears to dominate the solid state. Furthermore, the fact that the compound is EPR silent in the solid state implies that a diamagnetic compound exists as the primary species in the solid. It was proposed that a symmetrically bridging carbonyl  $[\text{Ta}(\text{CO})_4(\text{dppe})]_2$  dimer is responsible for the pairing of the radical electrons and the resulting diamagnetism. From the magnetic susceptibility measurements, the authors calculated  $\Delta H$ ,  $\Delta S$ , and  $\Delta G^{(213)}$  for dimerization of  $-4.0 \text{ kcal mol}^{-1}$ ,  $-12 \text{ cal mol}^{-1} \text{ K}^{-1}$ , and  $-1.4 \text{ kcal mol}^{-1}$ , respectively. However, due to the thermal instability of  $\text{Ta}(\text{CO})_4(\text{dppe})$ , crystalline samples

of the complex were not obtained, thereby precluding a crystallographic structure determination.

The goal of this study is to elucidate the geometry of the  $\text{Ta}(0)$  dimer and to explore the electronic structure of its carbonyl bridging system. Calculations were performed on the model monomer  $\text{Ta}(\text{CO})_6$  and several isomers of the corresponding dimer  $\text{Ta}_2(\text{CO})_{12}$ . The chelating ligand  $\text{PH}_2\text{CH}_2\text{CH}_2\text{PH}_2$  (ethylenediphosphine, edp) was added to simulate the effects of dppe complexation on the calculated species, and the phenyl groups were added to the latter calculation by molecular mechanics and single-point electronic energy calculations.

## Computational Methods

All electronic structure calculations in this work were performed with the Gaussian 94 program.<sup>3</sup> Frequency calculations and most geometry optimizations and energy calculations were carried out using the B3LYP density functional method, which includes the Becke<sup>4</sup> three-parameter (B3) exchange functional and the Lee–Yang–Parr<sup>5</sup> (LYP) correlation functional. Several geometry optimizations and energy calculations were performed utilizing second-order Møller–Plesset<sup>6</sup> perturbation theory (MP2), primarily with the intent of verifying the B3LYP results.

Three basis sets were employed for these calculations. The first, hereafter referred to as basis set 1, is the LANL2DZ basis, which includes the Huzinaga–Dunning<sup>7</sup> double- $\zeta$  basis set for the carbon and hydrogen atoms and the double- $\zeta$  basis

(3) Frisch, M. J.; Trucks, G. W.; Schlegel, H. B.; Gill, P. M. W.; Johnson, B. G.; Robb, M. A.; Cheeseman, J. R.; Keith, T.; Petersson, G. A.; Montgomery, J. A.; Raghavachari, K.; Al-Laham, M. A.; Zakrzewski, V. G.; Ortiz, J. V.; Foresman, J. B.; Cioslowski, J.; Stefanov, B. B.; Nanayakkara, A.; Challacombe, M.; Peng, C. Y.; Ayala, P. Y.; Chen, W.; Wong, M. W.; Andres, J. L.; Replogle, E. S.; Gomperts, R.; Martin, R. L.; Fox, D. J.; Binkley, J. S.; Defrees, D. J.; Baker, J.; Stewart, J. P.; Head-Gordon, M.; Gonzalez, C.; Pople, J. A. *Gaussian 94*, Revision D.4; Gaussian, Inc.: Pittsburgh, PA, 1995.

(4) Becke, A. D. *J. Chem. Phys.* **1993**, *98*, 5648.

(5) Lee, C.; Yang, W.; Parr, R. G. *Phys. Rev. B* **1988**, *37*, 785.

(6) Møller, C.; Plesset, M. S. *Phys. Rev.* **1936**, *46*, 618.

(7) Dunning, T. H.; Hay, P. J. In *Modern Theoretical Chemistry*; Schaefer, H. F., III, Ed.; Plenum: New York, 1976; pp 1–28.

(1) DeKock, R. L. *Inorg. Chem.* **1971**, *10*, 1205.

(2) Koeslag, M. A.; Baird, M. C.; Lovelace, S.; Geiger, W. E. *Organometallics* **1996**, *15*, 3289.

set of Hay and Wadt<sup>8</sup> for the phosphorus and tantalum atoms. Basis set 2 likewise used LANL2DZ, but, in the tantalum basis, the two outermost p-functions were replaced by a (41) split of the optimized outer p-function from Couty and Hall.<sup>9</sup> Basis set 3 was identical to basis set 2, except that polarization (d) functions have been added to the four carbonyl groups found in the bridging region.

Steric interactions initiated by the consideration of the full dppe chelating ligand were examined using the UNIVERSAL 1.02 force field as it is implemented in the Cerius2 program.<sup>10</sup> For each species, the phenyl groups were substituted onto the B3LYP-optimized geometry and allowed to optimize alone in the force field with respect to the rest of the structure. The energy of each of the geometries was then determined by a single-point energy calculation with the B3LYP method. The basis set used for these energy calculations was identical to basis set 1, except that Pople's STO-3G basis<sup>11,12</sup> was assigned to all of the carbon and hydrogen atoms in the dppe ligands.

To estimate the basis set superposition error (BSSE) in the most stable structures, the unchelated  $D_2$  dimer was examined in basis set 1 with the counterpoise method.<sup>13</sup> It is not surprising that this procedure found the BSSE to be as substantial as 6.1 kcal mol<sup>-1</sup>, because the counterpoise method assumes the monomer's distortion to be independent of the employed basis set. The same calculation using the more complete basis set 3 still exaggerated the BSSE but gave a smaller result of 5.4 kcal mol<sup>-1</sup>. Utilization of the counterpoise method for large, facile moieties frequently leads to an overestimation of the BSSE.

## Results and Discussion

**Monomer.** Most of the unchelated structures were derived from the octahedral model of Ta(CO)<sub>6</sub> and were calculated using basis set 1. A Jahn–Teller distortion from perfect  $O_h$  symmetry was inevitable for the expected  $t_{2g}^5$  low-spin electron configuration. From group theoretical arguments, it can be shown that the only Jahn–Teller active modes for a low-spin d<sup>5</sup>, octahedral system must be of either the  $e_g$  or  $t_{2g}$  symmetry type. The four structures (1–4) shown below and the structure shown in Figure 1 (5) all result from various linear combinations of these distortions. The ligands of structures 1 and 2 all lie along the Cartesian axes, whereas 3 and 4 have undergone angular distortions. Metal–carbon bond lengths are differentiated above by hash marks. Examination of optimized structures for 1–3 revealed that all exhibited at least one imaginary frequency, which indicates that further symmetry breaking would be necessary.<sup>14</sup> The geometry optimization of monomer 4 failed to meet the convergence criteria and was higher in energy than those for the other structures shown. All of the expected distortions led either to one of the other displayed geometries (1–5) or ultimately to a  $C_i$  structure similar in both energy and geometry to that of 5 (Figure 1).

Linear combination of any two of the three degenerate  $t_{2g}$  distortions in a 1:±1 ratio yields a structure of  $C_{2h}$

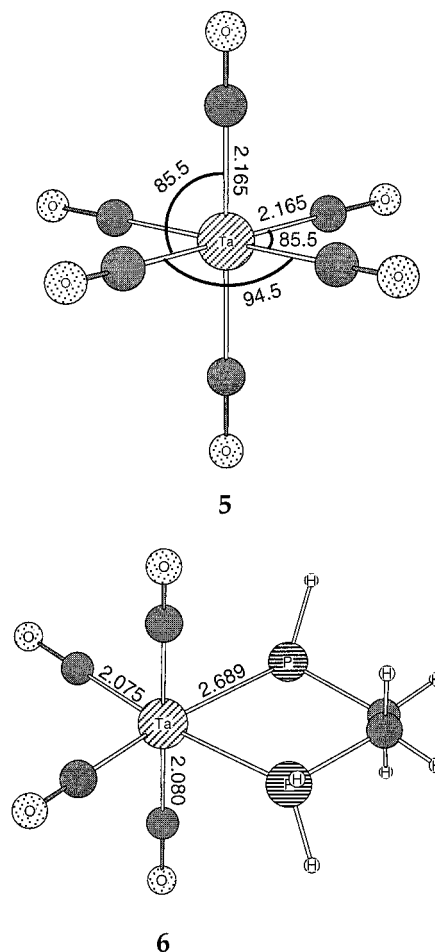
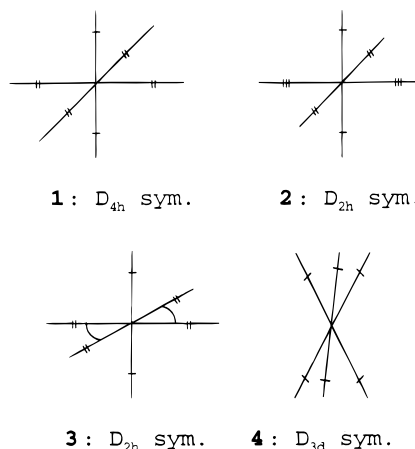


**Figure 1.** Stable monomers: **5** is the unchelated structure of  $C_{2h}$  symmetry and **6** is the edp-chelated structure of  $C_2$  symmetry.



symmetry (5). It exhibits all real frequencies and is lower in energy than any other Ta(CO)<sub>6</sub> structure. As can be seen in 5, the metal–carbon bond distances differ only very slightly in the two sets of symmetry non-equivalent carbonyls. This near-octahedral  $C_{2h}$  structure was concluded to be the stable, unchelated monomer.

The rotational axis of the molecule was preserved upon substitution of the edp ligand, yielding the near-octahedral  $C_2$  structure shown in Figure 1 (6). The chelated model was, according to frequency calculations,

(8) Hay, P. J.; Wadt, W. R. *J. Chem. Phys.* **1985**, *82*, 299.

(9) Couty, M.; Hall, M. B. *J. Comput. Chem.* **1996**, *17*, 1359.

(10) *Cerius2 User Guide*; Molecular Simulations Inc.: San Diego, April 1997.

(11) Hehre, W. J.; Stewart, R. F.; Pople, J. A. *J. Chem. Phys.* **1969**, *51*, 2567.

(12) Collins, J. B.; Schleyer, P. v. R.; Binkley, J. S.; Pople, J. A. *J. Chem. Phys.* **1969**, *51*, 2567.

(13) Hobza, P.; Zahradnik, R. *Chem. Rev.* **1988**, *88*, 871.

(14) Whereas 2 was never explicitly examined, frequency calculations performed on a structure with symmetry lowered from that of 2 revealed an imaginary frequency.

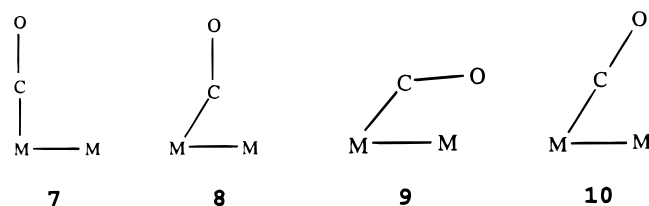
**Table 1.** Room-Temperature Solution IR Spectra in Toluene and Unscaled B3LYP Frequencies

frequency (cm <sup>-1</sup> )		intensity	
exp	calc	exp	calc (km mol <sup>-1</sup> )
1962	1939	medium	470
1891	1845	strong	1189
	1844		542
1878	1826	very strong	2395

also at a minimum on the energy surface. Calculations with basis set 2 yielded nearly identical results.

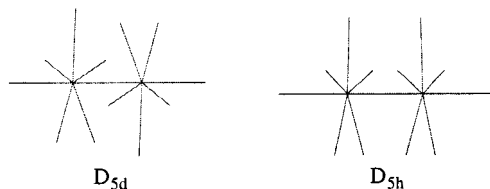
Shown in Table 1 are the experimental (room-temperature, solution-phase) and the theoretical IR carbonyl frequencies and intensities for Ta(CO)<sub>4</sub>(edp). These results were obtained with basis set 1 and remain unscaled. Comparison of the computed IR frequencies of Ta(CO)<sub>4</sub>(edp) to those experimentally observed for the monomeric Ta(CO)<sub>4</sub>(dppe) complex shows a good qualitative agreement between theory and experiment. This evidence strongly suggests that the calculated structure for the Ta(CO)<sub>4</sub>(edp) is a satisfactory model of the experimentally observed monomer.

**Unchelated Dimer.** A variety of carbonyl bridging forms have been previously observed and characterized.<sup>16–21</sup> It has become customary to classify bridging carbonyls as follows: terminal (7), bent semibridging (8), prone (9), and linear semibridging (10).



In an attempt to thoroughly explore the energy surface for any possible minima, structures exhibiting each of the major forms of carbonyl bridging were optimized and evaluated. This probe of the energy surface utilized the unchelated model Ta<sub>2</sub>(CO)<sub>12</sub>. Basis set 1 was used at the B3LYP level of theory.

Serving as the limiting case, nonbridging arrangements of *D*<sub>5d</sub> and *D*<sub>5h</sub> symmetry were investigated. These geometries, illustrated below, contain only terminal carbonyls (7). It was concluded from the optimi-



zations' failure to converge to a dimer with "normal" metal–metal bond lengths that the steric crowding created by such a large number of ligands prohibits the

(15) Churchill, M. R.; Amoh, K. N.; Wasserman, H. J. *Inorg. Chem.* **1981**, 20, 1609.

(16) Cotton, F. A. *Prog. Inorg. Chem.* **1976**, 21, 1.

(17) Crabtree, R. H.; Lavin, M. *Inorg. Chem.* **1986**, 25, 805.

(18) Sargent, A. L.; Hall, M. B. *Polyhedron* **1990**, 9, 1799.

(19) Benard, M.; Dedieu, A.; Nakamura, S. *Nouv. J. Chim.* **1984**, 8, 149.

(20) Morris-Sherwood, B. J.; Powell, C. B.; Hall, M. B. *J. Am. Chem. Soc.* **1984**, 106, 5079.

(21) Simpson, C. Q.; Hall, M. B. *J. Am. Chem. Soc.* **1992**, 114, 1641.

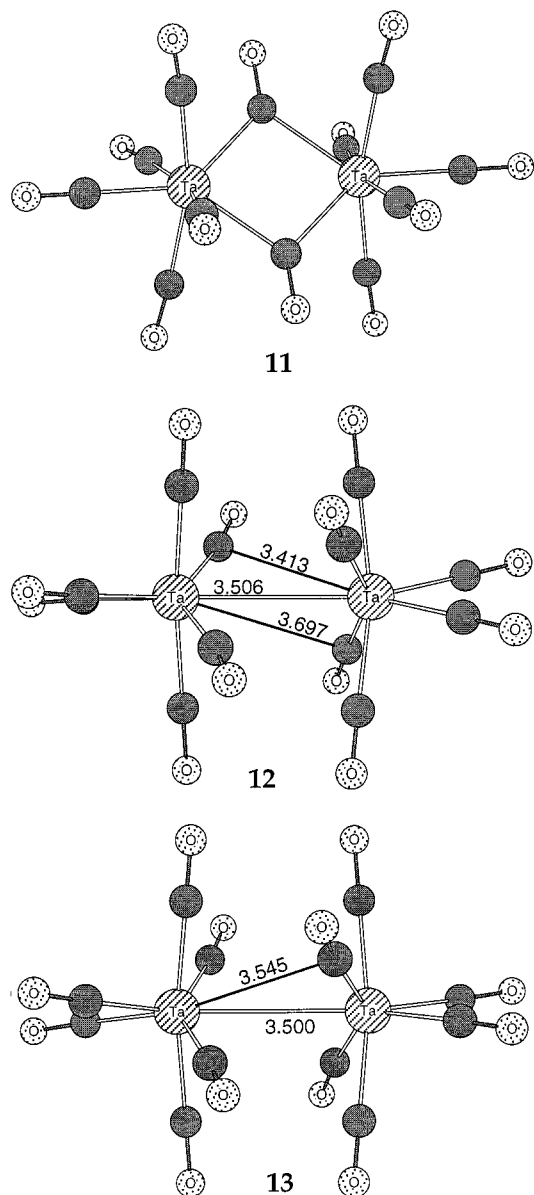


**Figure 2.** Unchelated dimers: **11** is a representative structure with symmetrically bridging bent carbonyls, **12** is a dibridged structure of *C*<sub>2</sub> symmetry, and **13** is a tetrabridged structure of *D*<sub>2</sub> symmetry. While all dimers exhibiting bent carbonyl bridges were found to be unfavorable with respect to dissociated monomers, both dimers exhibiting linear semibridging carbonyls were found to be energetically bound.

metal atoms from being close enough to form metal–metal bonds such as those of Mn<sub>2</sub>(CO)<sub>10</sub> or Re<sub>2</sub>(CO)<sub>10</sub>.<sup>15</sup> No nonbridged dimers were found to be energetically competitive with dissociated monomers.

Similarly unsuccessful were all attempts to find stable compounds containing bent semibridging (8) carbonyls. No critical points on the energy surface were found for those with unsymmetrical bent bridges, and all geometries with symmetrical bridging carbonyls (Figure 2, **11**) corresponded to energies prohibiting stable dimerization. These results are as anticipated, since bent semibridging carbonyls are more commonly seen for smaller metal atoms or for highly polar metal–metal bonds.<sup>16</sup>

Investigation of models in which prone (9) carbonyls act as four-electron donors likewise produced only high-



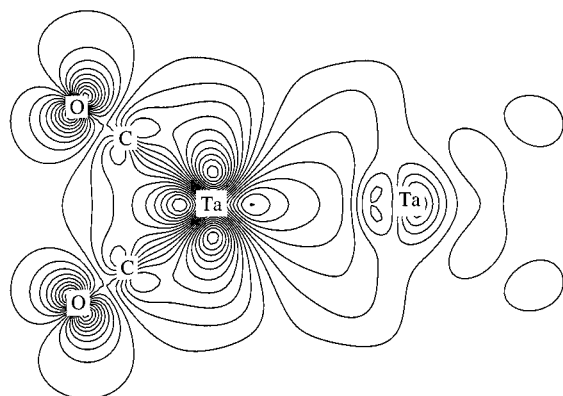
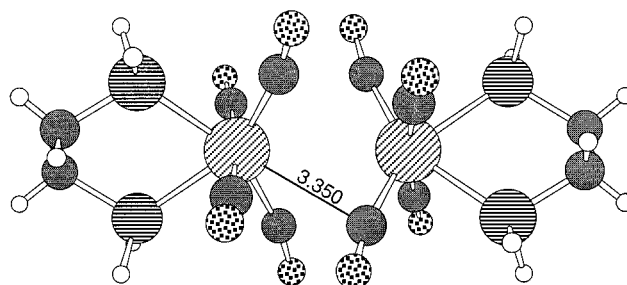


**Figure 3.** Bonding molecular orbital from the unchelated  $C_2$  dimer, exhibiting direct Ta–Ta bonding, supported by linear semibridging carbonyl character.

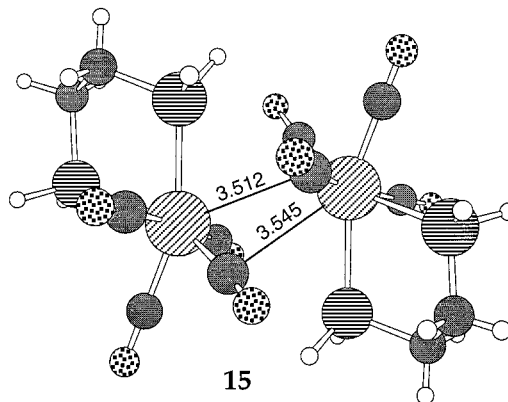
energy structures. The donations from the  $\pi$ -orbitals of these carbonyls are shown in studies by Crabtree and Lavin<sup>17</sup> and Sargent and Hall<sup>18</sup> to commonly occur only in complexes with early transition-metal secondary centers. The electron richness and steric hindrance of the secondary tantalum atom in the dimer  $Ta_2(CO)_{12}$  create an environment unlikely to support prone (9) carbonyl bridges.

A dimer of  $C_2$  symmetry containing two linear semibridging carbonyls (10) was found to be bound by  $2.4 \text{ kcal mol}^{-1}$  with respect to unassociated monomers (Figure 2, 12). Frequency calculations in basis set 1 indicate that this dibridged structure is a minimum in the energy surface. However, a geometrically similar tetrabridged dimer of  $D_2$  symmetry (Figure 2, 13) converged to within  $+0.07 \text{ kcal mol}^{-1}$  of its dibridged counterpart. Although the  $D_2$  model was shown in basis set 1 to exhibit a small imaginary frequency, geometry optimizations in basis set 3 of the two dimers maintained their subtle structural differences while giving a calculated energy difference of less than  $+0.03 \text{ kcal mol}^{-1}$ . In this more complete basis set, the calculated binding energy was found to increase to  $4.2 \text{ kcal mol}^{-1}$ . Although these competing models never fully optimized to identical geometries, it is quite possible that only one dimer exists in reality. The B3LYP theoretical method may be incapable of identifying or resolving the discrepancy on such a flat energy surface. The problem was further investigated with MP2 calculations on the competing geometries of  $C_2$  and  $D_2$  symmetry. Although the computations were not run to full convergence, it was clear that MP2 maintained their unique, isoenergetic geometries.

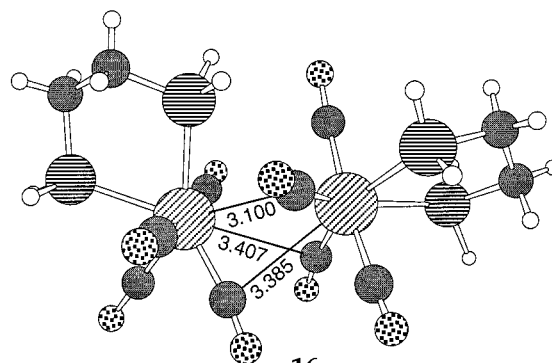
It is not altogether surprising that the dimer in question exhibits linear semibridging carbonyls. An examination of the orbital responsible for the binding of the monomers (Figure 3) leads to immediate support of the linear semibridging electronic description provided by Benard et al.<sup>19</sup> and Morris-Sherwood et al.<sup>20</sup> The in-phase interaction of the CO antibonding ( $\pi^*$ ) orbitals with the Ta–Ta metal bond yields the observed multicentered bonding orbital and logically satisfies the unusually large calculated metal–metal distance. A theoretical study by Simpson and Hall<sup>21</sup> concluded that the ultimate impetus for a linear semibridging carbonyl system is the alleviation of a steric strain in the ligand system. This conclusion implies that energetic fa-



14



15



16

**Figure 4.** Chelated dimers: (14)  $D_2$  symmetry, (15)  $C_1$  symmetry, and (16)  $C_1$  symmetry. All were found to exhibit linear semibridging carbonyls like those of the unchelated structures.

vorability of the tantalum–tantalum interaction drives the original dimerization, and the observed carbonyl bridges are merely an expression of the resulting steric crowding.

An estimate of the strength of the direct antiferromagnetic coupling between the two tantalum atoms can be obtained by calculation of the singlet–triplet energy separation. Using basis set 1, we found that the triplet state is less stable by 2.44 eV in the dimer of  $D_2$  symmetry. Because the antiferromagnetic coupling energy is so much greater than the binding energy of the dimer, it is not surprising that further optimization of the triplet geometry led the monomers to pull apart. The bulk of the triplet spin density is evenly distributed between the two metal atoms.

In a hypothetical scenario in which two of the terminal carbonyls on the bound dimer of  $C_2$  symmetry were removed and replaced by a 4– charge, the resulting optimization of  $[Ta_2(CO)_{10}]^{4-}$  relaxed to a completely nonbridging configuration like that of the isoelectronic

$\text{Re}_2(\text{CO})_{10}$ . Although such evidence may be interpreted to support the consideration of steric strain as the motive for linear semibridging, the problematic nature of ab initio calculations on molecules with a large negative charge may render this particular example little more than interesting.

**Chelated Dimer.** Three distinct chelated isomers were explored. The edp ligands utilized were simplified forms of the experimental dppe. The dimer geometries were optimized in basis set 1 to the structures **14**–**16** shown in Figure 4. The natures of the carbonyl bridging systems are all very similar. The expectation of linear semibridging carbonyls from examination of the unchelated species is maintained in each optimized isomer of the edp-substituted dimer. Whereas the  $D_2$  isomer **14** and the  $C_i$  isomer **15** are both tetrabridged, the  $C_1$  structure **16** has only three bridging carbonyls. The structures of the bridging system in both of the less symmetric models are easily seen as simple derivatives of the more highly symmetric  $D_2$  isomer, **14**, which further bears obvious resemblance to the calculated unchelated models. The variance in the bridging structure is most likely due to the response of the individual isomers to steric influences created by the edp's respective occupation of different coordination sites.

All three models have energies bound with respect to those calculated for the monomer. Isomer **16** is found to be the most stable, with a binding energy of 6.18 kcal mol<sup>-1</sup>, whereas isomers **14** and **15** are bound by 2.59 and 0.97 kcal mol<sup>-1</sup> respectively. The stabilities of the three structures are close enough to have their relative order subject to such factors as dppe-induced steric effects (considered below) and crystal packing effects.

Steric interactions initiated by the introduction of the phenyl rings to the chelating ligand were examined by optimizing their position on the fixed dimer frame and

recalculating the DFT energy. This analysis suggested that dimer **14** would be less inhibited by the presence of phenyl rings than either of the other two structures. Models **15** and **16** are respectively 9.3 and 24.4 kcal mol<sup>-1</sup> higher in energy than the more symmetric isomer **14**. Because the quality of this mixed DFT/force field geometry optimization limits the rigor of these calculations, the dimer is calculated to be unstable with respect to the chelated monomer. This deficiency could be overcome only by the full DFT optimization of the dimer. Despite these limitations, all the results, taken together, suggest that the weakly bound, experimentally observed dimer  $[\text{Ta}(\text{CO})_4(\text{dppe})]_2$  exhibits a geometry with linear semibridging carbonyls.

## Conclusion

This study has elucidated the electronic structure of the  $[\text{Ta}(\text{CO})_4(\text{dppe})]_2$  bridging system and proposed three somewhat similar structures for the chelated dimer. Although the energetic competition between these structures will most likely leave their relative abundance subject to sensitive external influences, there is strong evidence that any dimerized complex will be bound by linear semibridging carbonyls that support a weak, delocalized Ta–Ta interaction. By means of a thorough examination of the  $\text{Ta}_2(\text{CO})_{12}$  energy surface, it was found that no other method of interaction would lead to the favorable coupling of the  $\text{Ta}(\text{CO})_4(\text{dppe})$  radical monomers.

**Acknowledgment.** We thank the National Science Foundation (Grant Nos. CHE 94-23271 and CHE 95-28196) and the Robert A. Welch Foundation (Grant No. A-648) for financial support.

OM980144A